

온도 상승에 따른 압축강재의 좌굴 및 한계 판폭두께비

Buckling and Limit Width-Thickness Ratios of Steel Columns under Compression at Elevated Temperatures

강 성 덕*
Kang, Seong-Deok

김 재 익**
Kim, Jae-Uk

최 현 식***
Choi, Hyun-Sik***

요약

본 연구는 온도 증가에 따른 압축을 받는 H형 강재의 플랜지와 웨브의 국부 및 전체좌굴응력 내화해석 프로그램 개발과 플랜지와 웨브가 항복파괴전에 국부좌굴이 일어나지 않을 한계 판폭두께비의 상관값을 구하는 프로그램을 개발하는 것이다. 고온에서의 강재의 응력-변형도 관계식은 EC3:Part 1.2를 근거로 하였으며, 비교, 검토를 위하여 영국 BS5950의 강재를 대상으로 온도 증가에 따른 압축을 받는 강재의 플랜지와 웨브의 파괴온도와 하중을 본 연구의 내화해석 프로그램으로 예측하였다. 본 연구는 좌굴 및 항복에 대한 내화해석 프로그램을 개발하는 것을 목적으로 하고 적용 예를 통하여 좌굴 및 한계 판폭두께비를 분석하고 개발 프로그램의 타당성을 검토하였다.

키워드 : 좌굴계수, 온도상승, 좌굴응력도, 임계온도, 임계하중, 하중비

Keywords : buckling coefficient, elevated temperature, buckling stress, critical temperature, critical load, load ratio

1. Introduction

Steel structures are extensively used in industrial and civil engineering due to those own advantages as a relatively cheap material with fast erection, high strength and light weight. However, a big disadvantage of the steel as a structural material is its vulnerability to elevated temperatures. Under the fire condition, steel loses a considerable amount of strength and stiffness as its temperature rises and the overall and local buckling stress decreases at faster rate than yield stress at high temperatures. Therefore

the flange and web of steel universal columns, BS5950-Part1¹⁾, under compression can fail in the overall and local buckling at high temperatures.

Due to the non-linear stress-strain relationships of steel member at high temperatures in fire, the overall and local buckling behaviors become more complicated. However, there are very few theoretical studies with validation by experimental results of the flange and web of steel columns under compression at elevated temperatures. The fire analysis for the overall and local buckling of the flange and web of steel columns under compression at elevated temperatures is important because the experimental cost is very expensive.

Hancock studied the overall and local, distortional and flexural-torsional buckling of cold-formed steel at ambient temperature about their major axis²⁾. The method of analysis used herein is based on the finite strip method.

* Senior Associate, Division of Structural Design,
Hyundai Architects & Engineers Association, Seoul,
Korea

** Graduate student, Department of Architectural Eng.,
Keimyung University, Daegu, Korea

*** Corresponding author, Professor, Department of
Architectural Eng., Keimyung University, Daegu,
Korea,
E-mail : hsc261@kmu.ac.kr

Plank et al. studied the collapse analysis of steel columns in fire using an inelastic finite strip method³⁾. Bradford et al. studied the overall and local buckling of cold-formed steel of composite structural elements at elevated temperatures⁴⁾. By applying the principles of linear plate instability theory, to find critical loads, and the data found in EC3:Part 1.2⁵⁾, to evaluate the important material properties at elevated temperatures, the behavior of the beam in question has been evaluated. Jang et al studied the analysis of the yield stress and the deflection⁶⁾. Koo et al studied local and overall buckling of H-beams at elevated temperatures⁷⁾. Baik et al studied the local and overall buckling behavior of cold-formed channel columns under compression at elevated temperatures⁸⁾. Kang et al studied the local buckling and optimum width-thickness ratios of I-beans in fire⁹⁾. Design examples are analyzed by using the fire analytical program of this study and these results are compared with the fire analytical results by Wadee¹⁰⁾.

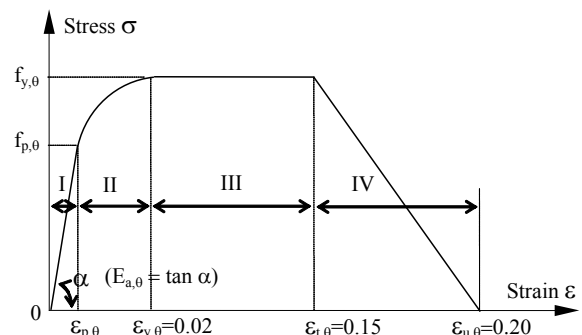
2. Material properties of steel at elevated temperatures

2.1 Stress-strain curves

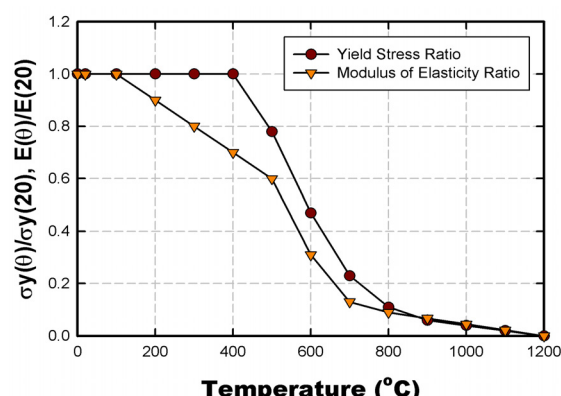
The structural steel is classified as SS400, SM490, S235, S275 and so on. The stress-strain relationship of the steel with grades S235, S275 and S355 (yield stress: MPa) is specified in EC3: Part 1.2 Annex A⁵⁾. The typical mechanical properties which show the perfect elasto-plastic behavior at ambient temperatures are well known. However, when exposed to fire, its material properties are changed and thermal expansion is induced. The high temperature stress-strain relationship of steel used herein is EC3: Part 1.2 model.

2.2 The EC3: model

The EC3:Part 1.2 presents the stress-strain relationship of the steel at elevated temperatures as a set of linear-elliptical curves as shown in <Fig. 1>. The form of the curve is divided into four ranges as summarized in <Table 1>. The relationship of yield stress and modulus of elasticity at elevated temperatures by EC3:Part 1.2 model is shown in <Fig. 2>. From 300°C steel begins to lose its strength and stiffness, and continues to lose strength at a fast rate until 750°C. Beyond this temperature, steel continues to lose its remaining strength at a slower rate until reaching its melting point (approximately 1500°C). Only 23% of the ambient-temperature strength remains at 700°C, and at 800°C this has reduced to 11% and at 900°C to 6%.



<Fig. 1> Stress-strain relationship for the steel at elevated temperatures



<Fig. 2> Ratio relationship of yield stress and modulus of elasticity at elevated temperatures by EC3

〈Table 1〉 Mathematical approximations of yield stress and modulus of elasticity at elevated temperatures by EC3

Strain range		Stress σ_θ	Tangent modulus E_t
I	elastic ($\varepsilon_\theta \leq \varepsilon_{p,\theta}$)	$E_\theta \cdot \varepsilon_\theta$	E_θ
II	transit elliptical ($\varepsilon_{p,\theta} \leq \varepsilon_\theta \leq \varepsilon_{y,\theta}$)	$\frac{b}{a} \sqrt{a^2 - (\varepsilon_{y,\theta} - \varepsilon_\theta)^2} + \sigma_{p,\theta} - c$ $a^2 = (\varepsilon_{y,\theta} - \varepsilon_{p,\theta})(\varepsilon_{y,\theta} - \varepsilon_{p,\theta} + c/E_\theta)$ <p style="text-align: center;">with $b^2 = E_\theta(\varepsilon_{y,\theta} - \varepsilon_{p,\theta})c + c^2$</p> $c = \frac{(\sigma_{y,\theta} - \sigma_{p,\theta})^2}{E_\theta(\varepsilon_{y,\theta} - \varepsilon_{p,\theta}) - 2(\sigma_{y,\theta} - \sigma_{p,\theta})}$	$\frac{b(\varepsilon_{y,\theta} - \varepsilon_\theta)}{a \sqrt{a^2 - (\varepsilon_{y,\theta} - \varepsilon_\theta)^2}}$
III	plastic ($\varepsilon_{y,\theta} \leq \varepsilon_\theta \leq \varepsilon_{t,\theta}$)	$\sigma_{y,\theta}$	0
IV	decreasing ($\varepsilon_{t,\theta} \leq \varepsilon_\theta \leq \varepsilon_{u,\theta}$)	$\sigma_{y,\theta} [1 - (\varepsilon_\theta - \varepsilon_{t,\theta}) / (\varepsilon_{u,\theta} - \varepsilon_{t,\theta})]$	---

where, σ_θ , $\sigma_{y,\theta}$, $\sigma_{p,\theta}$, E_θ are the stress, the yield stress, the proportional limit stress and the elastic modulus at temperature θ respectively;

$\sigma_{y,20}$, E_{20} are the yield stress and the elastic modulus at ambient temperature θ respectively;

ε_θ , $\varepsilon_{y,\theta}$, $\varepsilon_{p,\theta}$, $\varepsilon_{t,\theta}$, $\varepsilon_{u,\theta}$ are the strain, the yield strain, the proportional limit strain, the limiting strain for yield stress and the ultimate strain at temperature θ respectively;

In 〈Fig. 2〉, it can be seen that the modulus of elasticity decreases at faster rate than the yield stress and that the yield stress is almost invariable in about $\theta \leq 400^\circ\text{C}$ and decrease rapidly in about $400^\circ\text{C} < \theta \leq 800^\circ\text{C}$ and that the modulus of elasticity is almost invariable in about $\theta \leq 100^\circ\text{C}$ and decrease rapidly in about $100^\circ\text{C} < \theta \leq 800^\circ\text{C}$.

It can be also seen that the yield stress and modulus of elasticity are zero in about $\theta = 1200^\circ\text{C}$.

3. Overall and local buckling of SUC in fire

3.1. Overall and local buckling stress in elevated temperatures

The elastic overall and local buckling stresses for the flange and web of steel columns under compression at elevated temperatures are,

$$\sigma_{\text{eff},\theta} = \frac{k_f \pi^2 E_\theta}{12(1-\nu^2)(b/t_f)^2} \quad (1)$$

for local buckling stress of flange

$$\sigma_{\text{sw},\theta} = \frac{k_w \pi^2 E_\theta}{12(1-\nu^2)(d/t_w)^2} \quad (2)$$

for local buckling stress of web

$$\sigma_{\text{so},\theta} = \frac{\pi^2 E_\theta}{\lambda^2} \quad (3)$$

for overall buckling stress

$$\lambda = \frac{Kl}{i} \quad (4)$$

Where,

k_f , k_w are the local buckling coefficient of the flange and web;

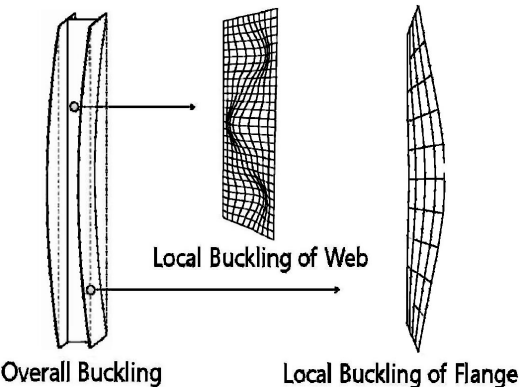
K is the buckling coefficient of column;

b , t_f are the width and thickness of the flange, mm;

d , t_w are the depth and thickness of the web, mm;

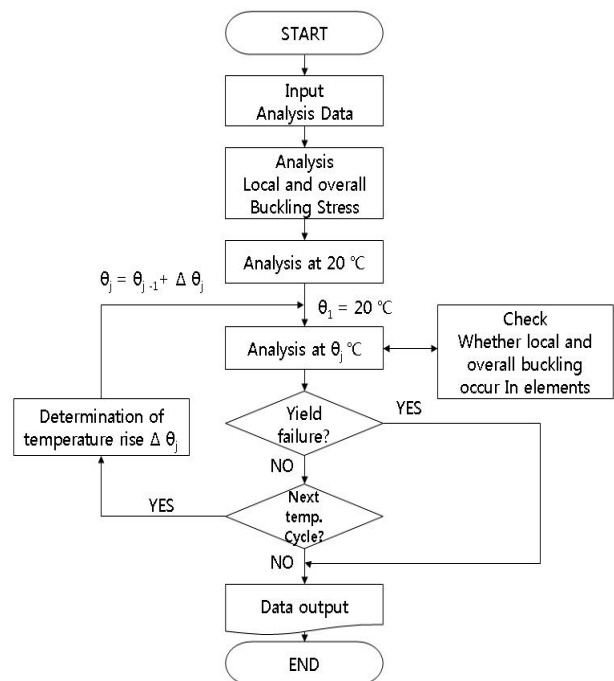
ν is Poisson's ratio for steel;
 E_θ is the modified modulus of elasticity of steel at temperatures θ , MPa;
 i and l are the ratio of gyration and height of column, mm.

In <Fig. 3>, buckled shape column compressed by the force at elevated temperature is shown. These mode shape are the overall and local buckling for the H-shaped steel section.



<Fig. 3> Mode shape of overall and local buckling

In this study, the computer program is developed to analyze the overall and local buckling stress of the flange and web of steel columns under compression at elevated temperatures based on Eqs. (1)-(4) and EC3: Part 1.2. <Fig. 4> is the flow chart for the fire analytical program of overall and local buckling stress of this study. Since one material may exist in a single column element, in order to facilitate the programming the steel H-shaped section concept has been employed with performance based on one material at ambient and elevated temperature.

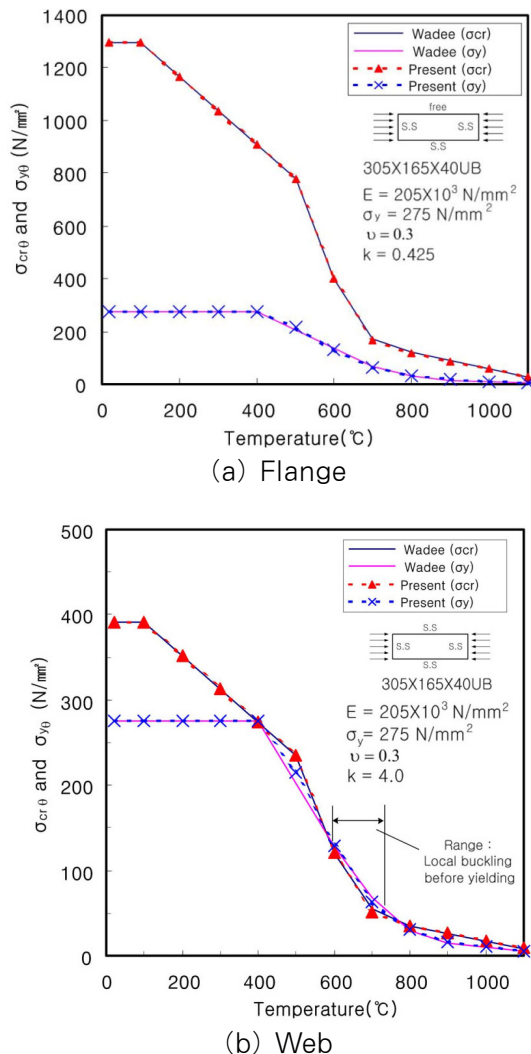


<Fig. 4> Flow chart for the fire analytical program of the overall and local buckling stress

3.2. Comparison between the results of computer analysis

<Fig. 5> represents the analytical results by Wadee and this study for the overall and local buckling stresses of the flange and web of 305x165x40UB under uniformly compression at elevated temperatures. In <Fig. 5>, "s.s" means simply supported end and "free" means free end.

In <Fig. 5>, it can be known that the present analytical results are good agreement with the analytical results by Wadee. In <Fig. 5>, it can be also seen that the overall and local buckling for the flange and web of steel columns under uniformly compression at elevated temperatures does not occur at flange in <Fig. 5(a)> but occurs at web in <Fig. 5(b)> prior to yield failure and that the critical temperature range of web is 575.0°C to 720.0°C in <Fig. 5(b)>.



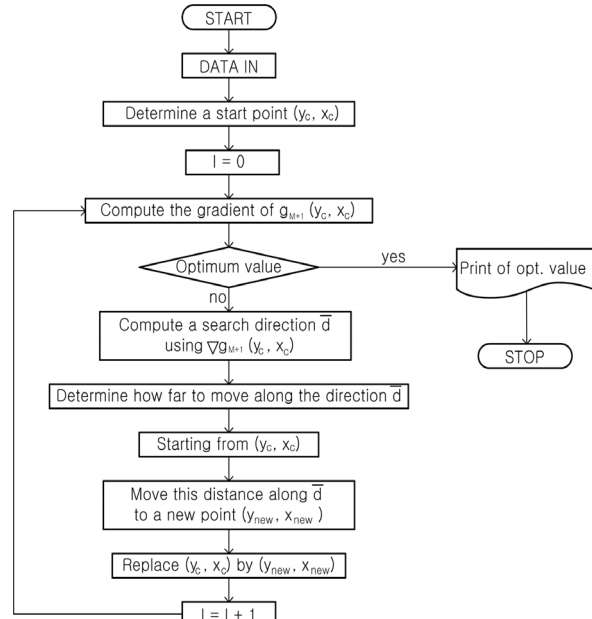
〈Fig. 5〉 Variations of the local buckling and yield stress of steel columns under compression at elevated temperatures

4. Optimization Formula for the Limit Slenderness Ratios in Fire

It is very important to find the limit width-thickness ratios, $(b/t_f)_{\lim}$ and $(d/t_w)_{\lim}$ for the flange and web of steel columns under compression at elevated temperatures that the overall and local buckling does not occur prior to yield failure.

In this study, the limit width-thickness ratios of the flange and web of steel columns under

compression at elevated temperatures considering the overall and local buckling can be easily calculated by using the non-linear optimum GINO(General Interactive Optimizer) program developed by Liebman et al¹¹⁾. <Fig. 6> is the flow chart of the optimum GINO Program



〈Fig. 6〉 The flow chart of the optimum GINO Program

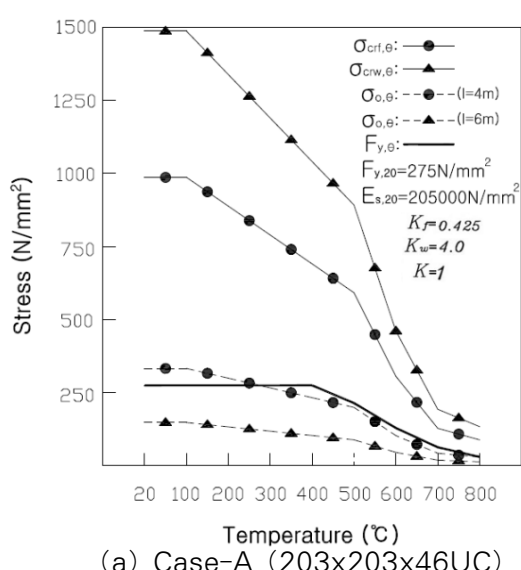
5. Design examples

The cross-section sizes of three steel columns are represented in <Table 2>. The design strength and elastic modulus at ambient temperatures were taken as 275 N/mm^2 and $205 \times 10^3 \text{ N/mm}^2$ respectively.

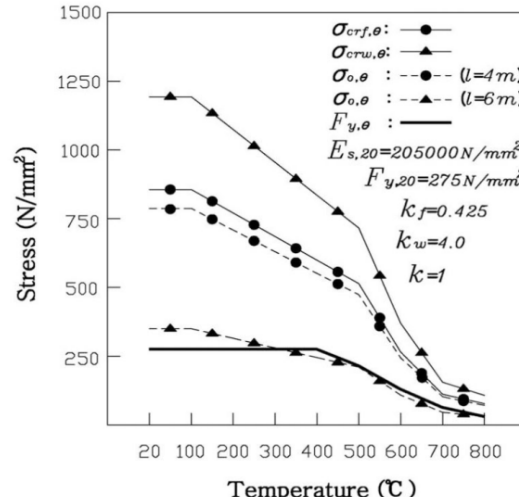
The overall and local buckling analysis of the flange and web of steel columns under uniformly compression at elevated temperatures is undertaken for temperatures of the following values, i.e. $\theta = 20, 100, 200, 300, 400, 500, 600, 700, 800^\circ\text{C}$. The flange width-thickness ratios are $b/t_f = 12, 14, 16, 18, 20$, and the web width-thickness ratios are $d/t_w = 40, 45, 50, 55, 60$. In <Table 2>, L.B is local buckling failure, O.B is overall buckling failure.

〈Table 2〉 Results of the critical temperatures and loads by load ratios for simply supported three H-shaped steel columns(SUC) under compression at elevated temperatures

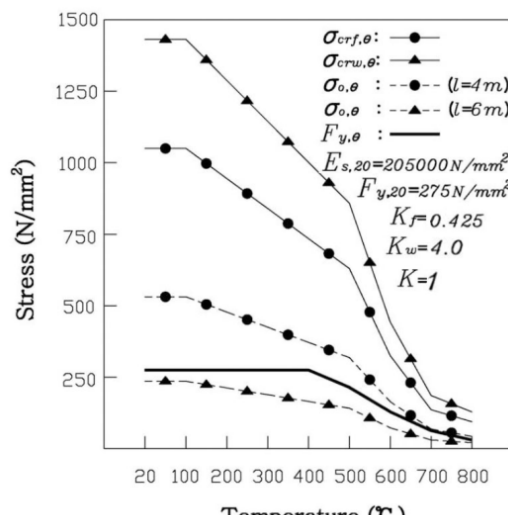
Column Size	Load Ratio	Critical Temperature	Critical Stress (N/mm ²)		Critical load (KN)		Remark	
			r	°C	4m	6m	4m	6m
Case-A (203x203x46UC)	0.5	590.3	112.5	50.0	660.3	293.5	L.B	O.B
	0.6	558.0	143.6	63.8	843.1	374.6	L.B	O.B
	0.7	525.3	175.2	77.9	1028.6	457.2	L.B	O.B
Case-B (254x254x73UC)	0.5	590.3	137.5	79.7	1280.1	742.7	Y	O.B
	0.6	558.0	165.0	101.8	1536.1	948.3	Y	O.B
	0.7	525.3	192.5	124.2	1792.2	1157.1	Y	O.B
Case-C (305x305x97UC)	0.5	590.3	137.5	118.5	1691.2	1458.5	Y	O.B
	0.6	558.0	165.0	127.7	2029.5	1571.5	Y	O.B
	0.7	525.3	192.5	172.9	2367.7	2127.5	Y	O.B



(a) Case-A (203x203x46UC)

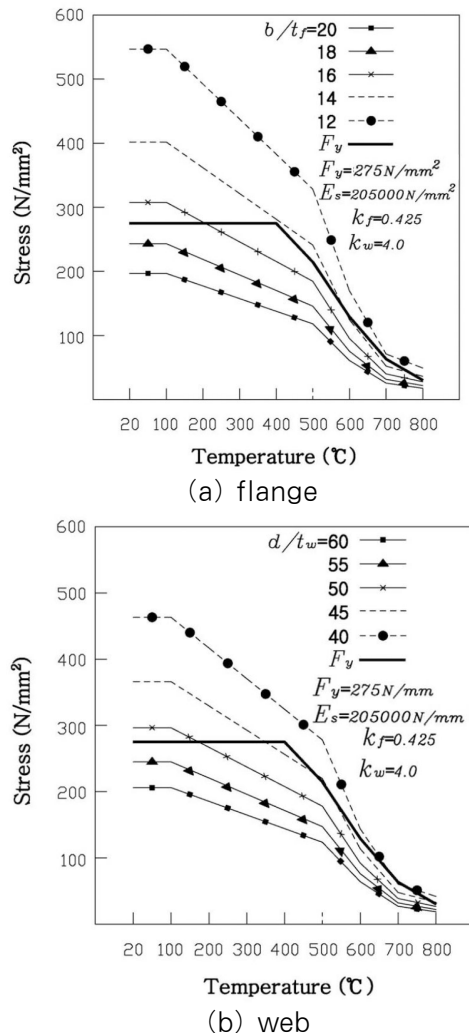


(b) Case-B (254x254x73UC)



(c) Case-C(305x305x97UC)

〈Fig. 7〉 Yield, overall and local buckling stresses of three steel columns under compression at elevated temperatures.



〈Fig. 8〉 Yield and local buckling stresses for flange and web under compression at elevated temperatures

〈Table 3〉 Results of the limit width-thickness ratios, $(b/t_f)_{\lim}$ and $(d/t_w)_{\lim}$ for the flange and web of steel columns under compression at elevated temperatures

Temperature (°C)	$(b/t_f)_{\lim}$				$(d/t_w)_{\lim}$			
	$k_f=0.425$		$k_f=1.28$		$k_w=4.0$		$k_w=6.8$	
	$\sigma_y (\text{N/mm}^2)$							
20	16.9	14.9	29.3	26.0	51.9	46.0	67.6	59.9
100	16.9	14.9	29.3	26.0	51.9	46.0	67.6	59.9
200	16.0	14.2	27.8	24.6	49.2	43.6	64.2	59.6
300	15.1	13.4	26.2	23.2	46.4	41.1	60.5	53.6
400	14.1	12.5	24.5	21.7	43.4	38.4	56.6	50.1
500	14.8	13.1	25.7	22.8	45.5	40.3	59.3	52.6
600	13.7	12.1	23.8	21.1	42.1	37.3	54.9	48.7
700	12.7	11.2	22.0	19.5	39.0	34.5	50.8	45.1
800	15.3	13.5	26.5	23.5	46.9	41.6	61.2	54.2

〈Fig. 8〉 shows the fire analytical results of the yield stress and the local buckling stress by the width-thickness ratios, b/t_f and d/t_w of the flange and web under compression at elevated temperatures.

〈Table 3〉 is the fire analytical results of the limit slenderness ratios, $(b/t_f)_{\lim}$ and $(d/t_w)_{\lim}$ for the flange and web of steel columns under uniformly compression at elevated temperatures. It can be also seen that the limit slenderness ratios of flange and web of steel columns between 20°C and 100°C.

In 〈Fig. 8〉 and 〈Table 3〉, it can be seen that the width-thickness ratios, $45 < d/t_w$ and $15 < b/t_f$ occur the local buckling and the slenderness ratios, $d/t_w \leq 45$ and $b/t_f \leq 15$ occur the yield in $F_y = 275 \text{ N/mm}^2$ and that the slenderness ratios, $40 < d/t_w$ and $13 < b/t_f$ occur the local buckling and the slenderness ratios, $d/t_w \leq 40$ and $b/t_f \leq 13$ occur the yield in $F_y = 350 \text{ N/mm}^2$.

6. Conclusions

The critical temperatures, critical loads and the limit width-thickness ratios for the flange and web of steel columns under compression at elevated temperatures are predicted by using the fire

analytical program of this study and the non-linear optimum GINO program. The H-shaped steel columns(SUC) under compression at elevated temperatures occurs mainly the overall and local buckling prior to the yield failure. The yield stress and modulus of elasticity of steel, buckling coefficients, and slenderness ratios are mainly affect for the overall and local buckling and the limit width-thickness ratios for the flange and web of steel columns in fire. A consistently good agreement with other analytical formulas shows that the proposed formulas can be utilized as a quick tool to access the compressive fire resistance of steel columns.

Acknowledgements

This research was supported by Basic Science Research Program through the National Research Foundation of Korea(NRF) funded by the Ministry of Education, Science and Technology (No.2011-0225).

References

1. Steel Design Guide to BS5950-Part1, 1990, The Steel Construction Institute.
2. Hancock, G.J. (1977), "Local and Overall, Distortional and Lateral Buckling of SHC," Research Report R312, University of Sydney, School of Civil Engineering, Sydney, Australia.
3. Olawale, A.O. and Plank, R.J. (1988), "The Collapse Analysis of Steel Columns in Fire Using a Finite Strip Method", International Journal for Numerical Methods in Engineering, 26.
4. Uy, B. and Bradford, M.A. (1995), "Local and Overall Buckling of Cold Formed Steel in Composite Structural Elements at Elevated Temperatures", Journal of Constructional Steel Research, 34.
5. European Committee for Standardization (CEN) (2000b), Eurocode3. Draft PrEN 1993-1-2, Eurocode3 : Design of Steel Structures, Part1.2 : General Rules, Structure Fire Design, British Standards Institution, London.
6. Jang, M.W., Kang, M.M. and Kang, S.D. (2003), "Stress and Deflection Analysis of Steel Beams at Elevated Temperatures", Journal of Korea Association for Shell and Spatial Structures, Vol. 3, No.1, pp.57-68.
7. Koo, B. Y., Kang, M.M. and Kang, S.D. (2004), "A Study on the Local and Overall Buckling at H-Beams at Elevated Temperatures", Journal of Korea Society of Steel Construction, Vol.16, No.1, pp.103-113.
8. Baik, T. S., Kang, S.D. and Kang, M. M.(2004), "Local and Overall Buckling Behavior of Cold-Formed Channel Columns under Compression at Elevated Temperatures", Journal of Korea Society of Steel Construction, Vol.16, No.1, pp.433-442.
9. Kang, M. M., Yun, Y. M., Kang, S. D. and Plank, R. T., "Local Buckling and Optimum Width-Thickness Ratios of I-Beans in fire", Journal of Korea Society of Steel Construction, Vol.17, No.4, 2005, pp.1-8.
10. Wadee, M.A. (1995), "Local and Overall Instability Phenomena in Fire", The Steel Construction Institute, RT533 Version 01.
11. Liebman, J., L.S. Lasdon, L. Schrage, L. Schrage and A. Waren (1986), Modeling and Optimization with GINO, The Scientific Press.

(접수일자 : 2012년 03월 30일)

(심사완료일자 : 2012년 08월 24일)

(게재확정일자 : 2012년 08월 31일)